Research article

Inhibition of circRNA NGFR promotes ferroptosis in gallbladder carcinoma cells

Desen Fan [1], Hui Liu [1], Bin Hu, Rongping Zhou, Changfeng Wang [**], Dong Yang [*]

Department of Gastroenterology and Pancreatic Surgery, The Affiliated Jiangning Hospital with Nanjing Medical University, Nanjing, Jiangsu, 211100, China

A R T I C L E   I N F O

A B S T R A C T

Background: Gallbladder carcinoma (GBC) is a formidably aggressive malignancy. Circular RNAs (circRNAs) play crucial regulatory roles in cancer. NGFR is a novel circRNA implicated in various types of cancers. The primary goal of this study was to elucidate the role of NGFR in GBC.
Methods: NGFR variants exhibiting discernible discrepancies were identified using RNA sequencing and validated using real-time PCR. Cell proliferation was assessed using 5-ethynyl-2′-deoxyuridine and Cell Counting Kit-8 assays. The ferroptotic phenotype was characterized by assessing the reactive oxygen species and Fe^{2+} levels. Western blotting was used to analyze ferroptosis-associated proteins. Superoxide dismutase, malondialdehyde, and glutathione levels were measured using commercially available reagent kits. The severity of mitochondrial damage was evaluated by assessing JC-1, MitoSOX, and ATP activities.
Results: NGFR was upregulated, and its suppression inhibited cell proliferation and increased Fe^{2+} levels in GBC cells. Furthermore, NGFR downregulation disrupted mitochondrial function.
Conclusion: Circular RNA NGFR can impede the advancement of GBC by modulating the ferroptotic phenotype, thereby potentially offering a novel avenue for the clinical diagnosis and treatment strategies of GBC.

1. Introduction

Gallbladder cancer (GBC) is the most common malignancy of the biliary tract. It accounts for 80–95 % of biliary tract cancers, ranking sixth on the global list of digestive tract cancers [1]. The risk factors for GBC include gallstones, gallbladder polyps (individual and symptomatic polyps >1 cm), chronic cholecystitis, obesity, and diabetes. Among these conditions, gallstones and chronic inflammation are the most common. Most adenocarcinomas are aggressive and are often detected late, leading to poor prognosis and less than 5 % five-year survival rate [2,3]. GBC is one of the most frequently observed malignant tumors in China.

Surgical resection is the main clinical method for GBC. Moreover, postoperative radiotherapy and chemotherapy can improve the prognosis. Targeted immunotherapy is a novel therapeutic strategy for the treatment of biliary malignancies. The best treatment plan

* Corresponding author. Department of Gastroenterology and Pancreatic Surgery, The Affiliated Jiangning Hospital with Nanjing Medical University, Nanjing, Jiangsu, 211100, China.
** Corresponding author. Changfeng Wang, Department of Gastroenterology and Pancreatic Surgery, The Affiliated Jiangning Hospital with Nanjing Medical University, Nanjing, Jiangsu, 211100, China.
E-mail addresses: jordanjordan@126.com (C. Wang), yangdongabp0@163.com (D. Yang).
[1] These authors have contributed equally to this work.

for GBC remains unclear; however, the development of new treatment methods is promising for improving patient survival.

Ferroptosis, a form of programmed cell death that differs from apoptosis, necrosis, and autophagy [4,5], was discovered in 2021 by Stockwell, a professor at Columbia University. Ferroptosis has attracted considerable attention and is associated with tumor cell death and inflammatory bowel disease [6,7]. Studies have shown that the development of diseases can be inhibited by activating or inhibiting ferroptosis. Identifying the key indicators of ferroptosis and understanding the relationship between ferroptosis and their development of diseases will offer new insights into preventing and treating diseases [8–10].

CircRNAs are noncoding RNA. They are produced by reverse shear through non-classical shear [11]. CircRNAs play important roles in various cancers, including drug resistance, epithelial-mesenchymal transition (EMT), and proliferation [12,13]. Moreover, circRNAs are related to various cancers. For example, circRNA 0000285 is expressed in cervical cancer [14], WHSC1 participates in endometrial cancer via miRNA-646 and NPM1 [15], and circRNA 001783 controls the progression of breast cancer [16]. The circRNA NGFR is a recently discovered circular RNA whose function, role, and mechanism of action in GBC remain unclear.

To clarify the pathogenesis of GBC from a new perspective and to discover new avenues and targets for its prevention and treatment, our study focused on investigating the impact of NGFR RNA as a novel molecular target for the clinical diagnosis and treatment of GBC.

2. Method and material

2.1. RNA-sequencing (RNA-seq)

RNA-seq was performed as previously described [17]. RNA was extracted from the tissues and used for RNA-seq to identify differentially expressed circRNAs. The DESeq R package was used for differential expression analysis between the two groups. The FDR was controlled using the Benjamini-Hochberg method. The cutoffs for identifying differentially expressed circRNAs were

$$| \log2 [FC] | > 1 \text{ and FDR } p < 0.05$$

2.2. Cell culture and treatment

The HGBECs and GBC cells (GBC-SD, NOZ, and SGC-996) were purchased from American Type Culture Collection (ATCC) (Virginia, United States). The cells were cultured in MEM medium (Sigma Chemical Co., St Louis, MO, USA) containing 1 % P/S and 12 % FBS (Gibco Laboratories, NY, USA) at 37 °C in a 5 % CO_2 environment. The cells were treated in six groups: sh-NC, sh-NGFR, sh-NGFR + Z-VAD, sh-NGFR + CQ, sh-NGFR + Nec-1, and sh-NGFR + Fer-1.

2.3. Cell transfection

To knock down the expression of NGFR, we used shRNA for NGFR (sh-NGFR:5′-UAAUAUUCUCCCUUUUUUGAU-3′). Non-specific controls (sh-NC: F-5′-CCGUUGAAAGGCCUACCCUCA-3, ′R-5′-UGAGGGUAGGCCUUUCAACGG-3′) were obtained from Thermo Fisher Scientific (Waltham, MA, USA). All sequences were transfected into cells using the JETPrime software (Polyplus, France). After 48 h, cells were collected for cell function and gene expression analyses.

2.4. qPCR

RNAs were extracted using the TRIzol reagent (Beyotime Company, Beijing, China). cDNA was synthesized from RNA using an RT-PCR kit (Yeasen, China), and qRT-PCR was conducted using the SYBR qPCR Mix (Vazyme, Nanjing). The PCR was performed using an ABI 7900 fluorescence quantitative PCR instrument (ABI, USA). The expression of β-actin was applied to standardize mRNA expression and use the variation $= 2^{-\Delta\Delta CT}$ method calculation. The primers of NGFR and β-actin were as follows: β-actin: 5′-AGAGCTAC-GAGCTGCCTGAC-3′(F) and 5′- AGCACTGTGTTGGCGTACAG-3′ (R), NGFR: 5′-CAGGTGTGGATCTTTCGTAATCA-3′ (F) and 5′-GTCCGGGTGTGGTAAAACAGG-3′ (R), HO-1:5′-AAGACTGCGTTCCTGCTCAAC-3′ (F) and 5′-AAAGCCCTACAGCAACTGTCG-3′ (R), and FTH: 5′-CCCCCATTTGTGTGACTTCAT-3′ (F) and 5′-GCCCGAGGCTTAGCTTTCATT-3′ (R). Initiating with an initial denaturation stage lasting 10 min at 95 °C, the process progressed through 40 cycles of denaturation at 95 °C for 10 s, annealing at 52.8 °C or 56.2 °C for 15 s, and extension at 72 °C for 20 s. The temperature gradient ranged from 72 °C to 95 °C, increasing in increments of 1 °C per step; the gain calibration was set before the first run.

2.5. EdU assay

Cell proliferation was determined using the EdU assay. Each common focus piece contained a 1×10^6 battery. EdU (50 μM) was used as the buffer, and cells were cultured at 37 °C for 120 min. The cells were immobilized using 4 % polyvinyl alcohol (PVA) as the carrier, followed by treatment with 0.1 % TritonX-100. Nucleic acids were stained with DAPI; growth rates were determined by analyzing images using Image J software (V1.8.0, NIH, Bethesda, Maryland, USA).

2.6. Cell-counting kit-8 (CCK-8)

Cells were seeded in a 96-well plate and cultured in DMEM/F12 medium at 37 °C and 5 % CO_2. After 24 h of treatment, cell proliferation was assessed using a CCK-8 kit (Beyotime Company, Beijing, China). The optical density (OD) was measured at 450 nm using a microplate reader (Bio-Rad Microplate Reader 550). Each experiment was repeated three times.

2.7. Measurement of MDA, SOD, GSH, and ATP activities

Malondialdehyde (MDA), superoxide dismutase (SOD), glutathione (GSH), and ATP levels were measured using activity kits (Jiancheng, Nanjing, China). The optical density (OD) of each well was measured at 525 nm according to the manufacturer's instructions.

2.8. Reactive oxygen species (ROS) assay

An ROS kit (Beyotime Company, Beijing, China) was used to quantify the ROS concentration. The absorbance was measured at 525 nm using a spectrophotometer (Cary 50, Varian Company, USA) following the manufacturer's protocol.

2.9. Iron detection

The cell lysate was harvested and used to determine the Fe-ion concentration. An iron detection kit (R&D Systems) was used, according to the manufacturer's instructions.

2.10. JC-1 assay

First, the cells were cultured at 37 °C and 5 % CO_2 at a denisty of 2×10^5 cfu/well. Next, we added 0.5 mL JC-1-dye working solution to it and incubated it at 37 °C for 30 min. The cells were then treated with DAPI at 37 °C for 20 min. Stained cells were observed and photographed under a microscope.

2.11. MitoSOX fluorescence assay

MitoSOX probes were purchased from the University of Shanghai (Shanghai, China). Briefly, cells were treated with the MitoSOX probe and then transfected with NGFR shRNA. After 48 h, the fluorescence intensity of the cells was observed under a fluorescence microscope (CKX53; Nikon).
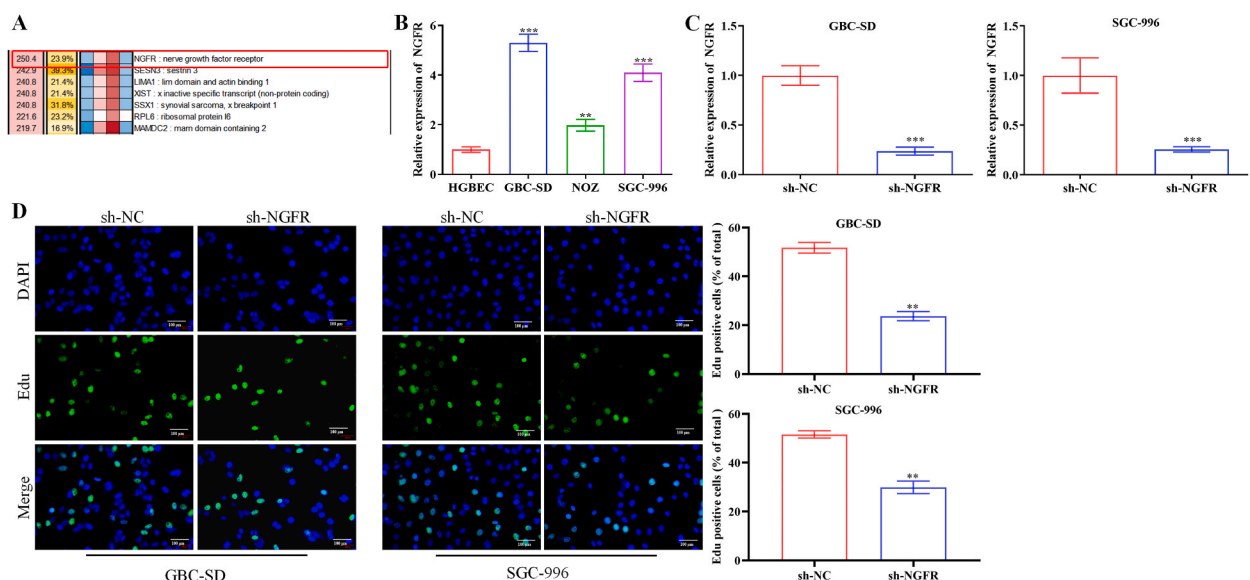

Fig. 1. Level of circRNA NGFR in gallbladder carcinoma (GBC). (A). Results of RNA-seq. (B). Level of circRNA NGFR in cancer cells. **$p < 0.01$, ***$p < 0.001$ vs HGBEC cells. (C). Efficiency of sh-NGFR transfection in GBC-SD and SGC-996 cells. ***$p < 0.001$ vs. sh-NC (D). Proliferation detected by EdU assay in GBC-SD and SGC-996 cells. **$p < 0.01$ vs. sh-NC. Data are expressed as mean ± SD of triplicate experiments.

2.12. Western blot

The proteins were transferred onto polyvinylidene difluoride (PVDF) membranes and blocked with 5 % skim milk. The PVDF membrane was then incubated overnight at 4 °C with the following specific primary antibodies for 12 h: SLC7A11 (ARG57998, Arigo), SLC3A2 (ARG43270, Arigo), GPX4 (ARG41400, Arigo), HO-1 (ARG54649, Arigo), FTH (ARG41439, Arigo), and actin (ARG62346, Arigo). The next day, the cells were blocked with secondary antibodies (SA00001-1, SA00001-2, Proteintech, China). The blots were visualized using enhanced chemiluminescence. β-actin was used as an internal reference protein. Protein expression was quantified using ImageJ software (V1.8.0, NIH, Bethesda, Maryland, USA).

2.13. Statistical analysis

The data obtained were analyzed using SPSS statistical software (IBM, Armonk, NY, USA). Continuous data were added and subtracted from the average, and the standard deviation was calculated. Statistical analyses were performed using the t-test, one-way ANOVA, and LSD tests to compare the groups. Values of $p < 0.05$ were considered statistically significant.

3. Results

3.1. NGFR was upregulated in GBC

To identify the key genes influencing the progression of GBC and to assess their expression, we used RNA-seq for gene discovery and qPCR for confirmation. RNA-seq revealed notable variations in circRNA NGFR across the groups (Fig. 1A). To validate these RNA-Seq findings, qPCR was used to quantify NGFR levels in GBC cells. The mRNA levels of NGFR increased in cancer cells, notably in GBC-SD
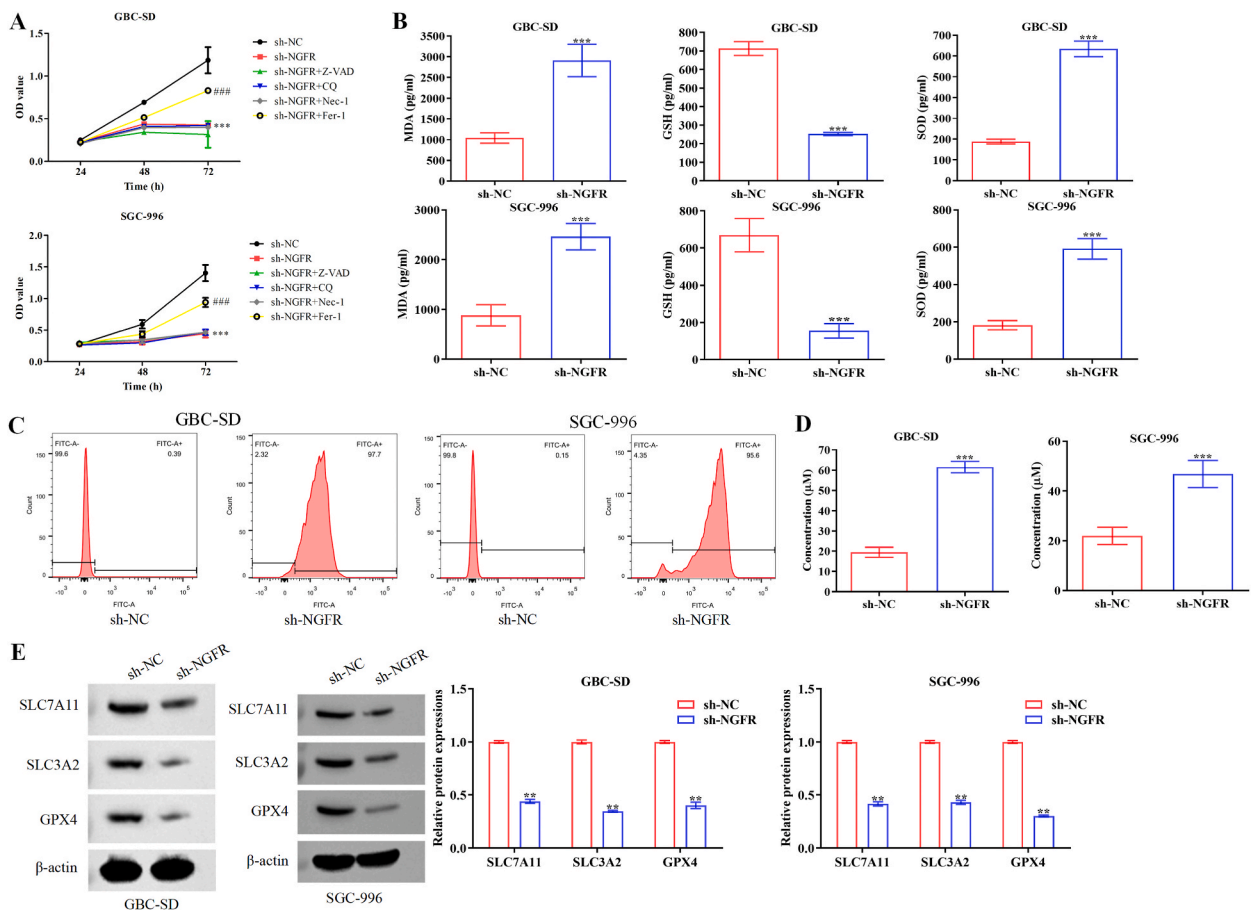

Fig. 2. Effect of circRNA NGFR on GBC cells. (A). Cell viability was calculated by CCK-8 in GBC-SD and SGC-996 cells. ***$p < 0.001$ vs. sh-NC, ###$p < 0.001$ vs. sh-NGFR. (B). Activity of SOD, MDA, and GSH in GBC-SD and SGC-996 cells. ***$p < 0.001$ vs. sh-NC. (C). ROS level determined by ROS assay kit in GBC-SD and SGC-996 cells. (D). Accumulation of Fe^{2+} was measured by the iron ion assay kit in GBC-SD and SGC-996 cells. ***$p < 0.001$ vs. sh-NC. (E). Expression level of ferroptosis-related protein in GBC-SD and SGC-996 cells. **$p < 0.01$ vs. sh-NC. Data are expressed as mean ± SD of triplicate experiments.

and SGC-996 cells (Fig. 1B). The efficacy of sh-NGFR was evaluated using qPCR, revealing reduced NGFR levels after sh-NGFR transfection (Fig. 1C). EdU results suggested that cell proliferation was halted following sh-NGFR transfection (Fig. 1D).

3.2. Inhibition of NGFR-induced GBC ferroptosis

The effect of shNGFR on cell proliferation was evaluated using the CCK-8 assay. Upon treatment with both sh-NGFR and a ferroptosis inhibitor, cell proliferation was restored. Conversely, when apoptosis, autophagy, and necrosis inhibitors were combined, cell proliferation remained unaffected (Fig. 2A), indicating that sh-NGFR impedes cancer cell proliferation by triggering ferroptosis. To substantiate this claim, we monitored the activities of SOD, MDA, and GSH and found that SOD and MDA levels were increased, and GSH activity was disrupted (Fig. 2B). Elevated ROS levels were observed in cells treated with sh-NGFR (Fig. 2C), along with increased accumulation of Fe^{2+} in the sh-NGFR group compared to that in the sh-NC group (Fig. 2D). Western blot analysis of ferroptosis-related proteins revealed the downregulation of xCT (SLC7A11 and SLC3A2) and GPX4 in the sh-NGFR group (Fig. 2E). These observations indicated that sh-NGFR suppressed cancer cell activity by inducing ferroptosis.

3.3. Damage to mitochondria induced by sh-NGFR

Ferroptosis is associated with mitochondrial impairment. To investigate the mitochondrial damage induced by sh-NGFR, we conducted experiments that yielded the following results. In comparison with the findings from the sh-NC group, the intensity of green fluorescence from JC-1 increased in the sh-NGFR group, accompanied by a decrease in red fluorescence (Fig. 3A). Fig. 3B illustrates an increase in MitoSOX fluorescence in the sh-NGFR group. Furthermore, ATP production in the sh-NGFR group decreased (Fig. 3C), implying that sh-NGFR has the potential to induce mitochondrial damage.

3.4. NGFR affected cell ferroptosis via the HO-1/FTH signaling pathway

Real-time PCR and western blotting were used to investigate the downstream genes and proteins in the HO-1/FTH signaling pathway influenced by NGFR in GBC-SD and SGC-996 cells. qPCR revealed an increase in the mRNA expression of HO-1 and FTH following sh-NGFR transfection (Fig. 4A). The protein levels of HO-1 and FTH increased in the sh-NGFR group (Fig. 4B), indicating the
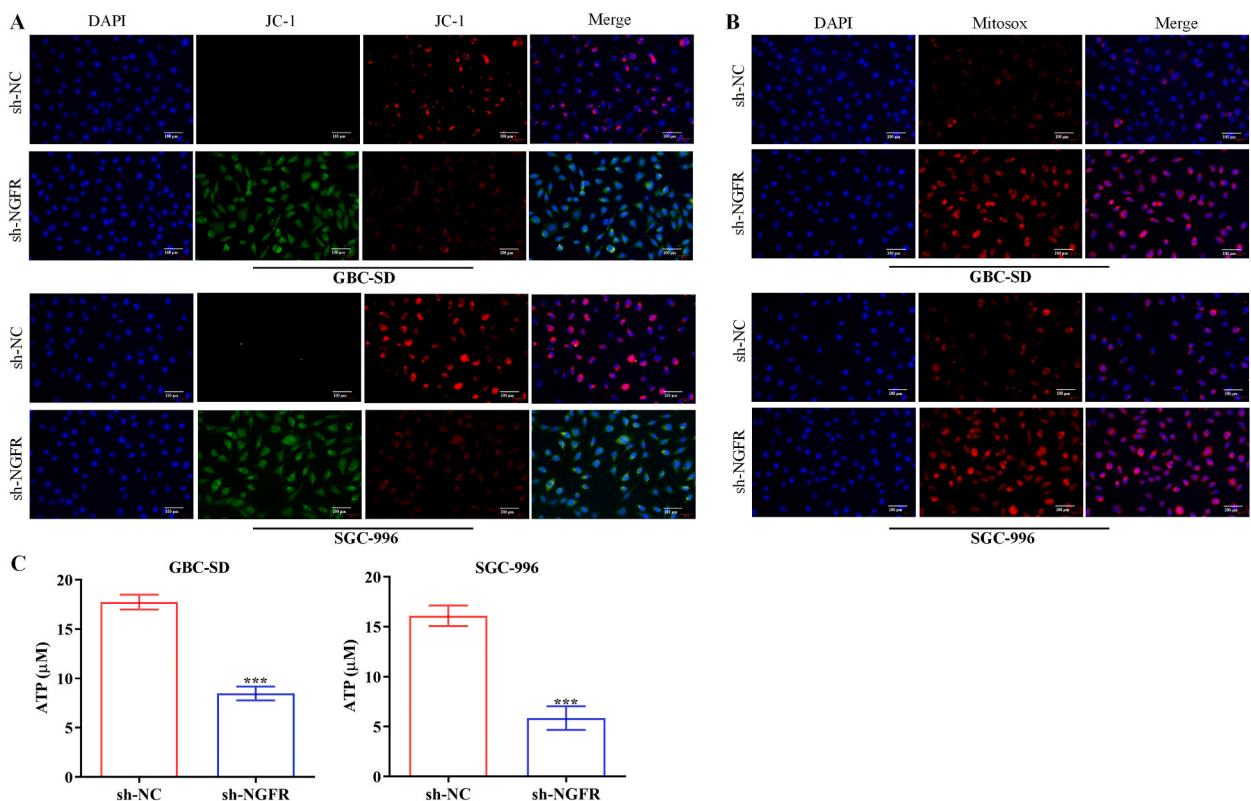

Fig. 3. Effect of NGFR on cancer-cell mitochondria. (A). Change in JC-1 fluorescence of GBC-SD and SGC-996 cells. (B). Fluorescence intensity of MitoSOX in GBC-SD and SGC-996 cells. (C). Concentration of ATP in GBC-SD and SGC-996 cells. ***$p < 0.001$ vs. sh-NC. Data are expressed as mean ± SD of triplicate experiments.
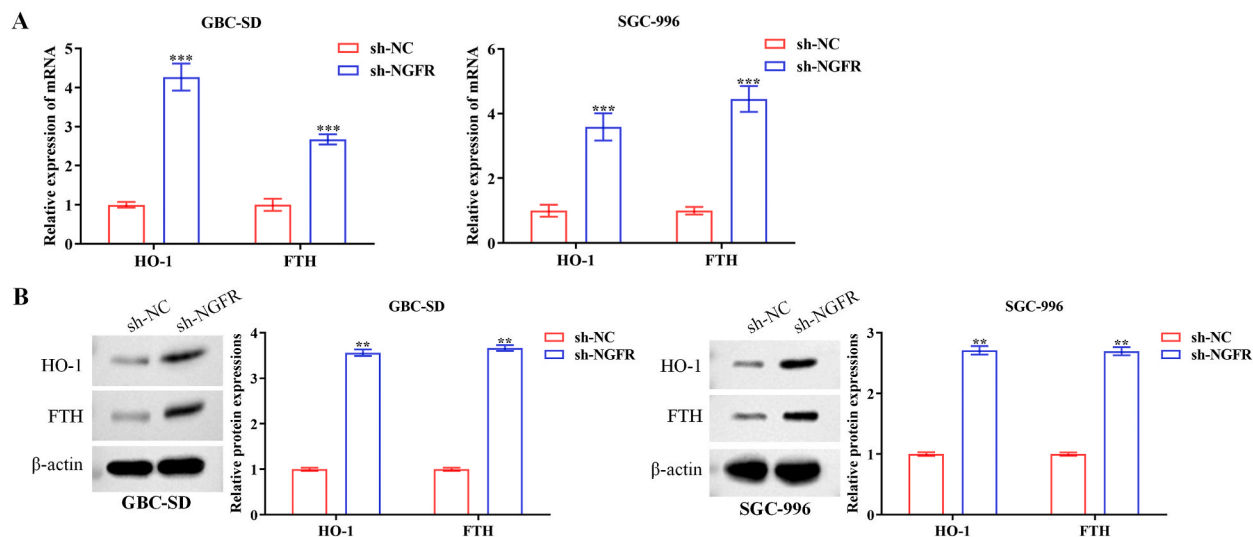
Fig. 4. Inhibition of NGFR-induced ferroptosis via HO-1/FTH signaling on GBC. (A). mRNA level of HO-1/FTH measured by qPCR in GBC-SD and SGC-996 cells. ***$p < 0.001$ vs. sh-NC. (B). Protein level of HO-/FTH detected by WB in GBC-SD and SGC-996 cells. **$p < 0.01$ vs. sh-NC. Data are expressed as mean ± SD of triplicate experiments.

involvement of the HO-1/FTH signaling pathway in NGFR-induced ferroptosis.

4. Discussion

GBC is highly invasive and prone to lymph node metastasis, direct infiltration of liver tissue, and intra-abdominal and blood metastases. The prognosis for this condition is generally poor, with a five-year survival rate of less than 5 % and a high fatality rate. The average survival time is typically 5–8 months. The long-term effects are worse than those of liver and pancreatic cancers, known as the "kings of cancer" [18]. Moreover, early GBC shows no obvious symptoms in the vast majority of malignant tumors. The coexistence of gallbladder stones and chronic cholecystitis is often observed. Notably, many patients often perceive themselves to have a "stomach disease." Oral drug treatment at home hinders patients from receiving medical attention, making early diagnosis of GBC difficult. Patients with gallstones, cholecystitis, or gallbladder polyps can also experience repeated attacks of right upper abdominal pain and other chronic gallbladder inflammations. When combined with gallstones, these symptoms should be treated promptly. If the disease develops into the middle or late stages, emaciation, fatigue, abdominal distension, jaundice, and a right upper abdominal mass are commonly observed.

The adoption of a GBC treatment method is also a matter of great concern. Similar to the vast majority of malignancies, surgical removal of tumors is the only possible cure for GBC, offering patients a long-term chance of survival [19]. Targeted therapies and immune checkpoint inhibitors have recently become popular topics in cancer treatment research. However, no satisfactory targeted drugs or immunosuppressants are currently available for the treatment of GBC. Many areas of tumor treatment need to be explored in clinical studies and scientific research.

The upregulation of NGFR in GBC cells indicates its potential impact on cancer progression. In this study, inhibition of NGFR demonstrated an inhibitory effect on cell proliferation, especially through ferroptosis induction. Notably, when ferroptosis is impaired, cell proliferation is reversed. Alterations in SOD, MDA, and GSH activities, as well as an increase in ROS levels, further substantiate the involvement of ferroptosis.

The essence of ferroptosis is glutathione peroxidase (Gpx4) function failure, leading to a decline in glutathione reductase (Gpx4) function, resulting in fat oxidation that cannot be degraded by its catalytic bivalent iron (Gpx4) and adipose tissue ferroptosis [20]. Many studies have shown that ferroptosis is associated with the inhibition of tumor progression. Wei et al. reported that tagitinin C induces ferroptosis in colorectal cancer (Cx1 RC) via the Nrf2/HO-1 axis [21]. Wang et al. identified ferroptosis-associated genes in breast cancer [22]. Ouyang et al. indicated that the inhibition of STAT3 repressed gastric-cancer-cell growth by inducing ferroptosis [23]. Another study confirmed that ketamine affected liver cancer cells by inducing ferroptosis [24]. Additionally, the modulation of ferroptosis-related proteins, such as xCT and GPX4, highlights the mechanism by which sh-NGFR hampers cancer cell activity. These results collectively underscore the role of NGFR in GBC development and the potential therapeutic implications of targeting ferroptotic pathways.

CircRNAs are important regulatory molecules involved in GBC progression and are important tumor markers in GBC. FOXP1 enhances GBC progression via PKLR signaling [25], and circRNAs are involved in the promotion of GBC. Researchers have suggested that inhibition of circRNA SMAD2 suppresses the growth of GBC through eIF4A3 [26]. However, there are few reports on the role of the circRNA NGFR in GBC development. Our previous study confirmed that NGFR was significantly overexpressed in GBC. Investigation of the mitochondrial damage induced by sh-NGFR in GBC cells revealed alterations indicative of mitochondrial dysfunction, including

changes in JC-1 and MitoSOX fluorescence and reduced ATP output. These findings suggest a potential link between NGFR expression and mitochondrial impairment. Furthermore, the upregulation of HO-1 and FTH at both the mRNA and protein levels following sh-NGFR transfection implied the involvement of the HO-1/FTH signaling pathway in NGFR-mediated cell ferroptosis.

In conclusion, our findings show that inhibition of circRNA NGFR modulates the phenotype of ferroptosis to repress the GBC process. Thus, circRNA NGFR may provide a new treatment strategy for GBC.

Availability of data and materials

The dataset used and/or analyzed in this study is available from the corresponding author on reasonable request.

CRediT authorship contribution statement

Desen Fan: Writing – review & editing, Writing – original draft, Methodology, Investigation, Conceptualization. **Hui Liu:** Writing – review & editing, Writing – original draft, Methodology, Investigation, Conceptualization. **Bin Hu:** Formal analysis, Data curation. **Rongping Zhou:** Writing – review & editing, Writing – original draft, Validation, Project administration, Funding acquisition, Data curation, Conceptualization. **Changfeng Wang:** Formal analysis, Data curation. **Dong Yang:** Writing – review & editing, Writing – original draft, Validation, Project administration, Funding acquisition, Data curation, Conceptualization.

Declaration of competing interest

The authors declare that they have no known competing financial interests or personal relationships that could have appeared to influence the work reported in this paper.

Acknowledgments

Appendix A. Supplementary data

Supplementary data to this article can be found online at https://doi.org/10.1016/j.heliyon.2024.e30260.

References

[1] R. Hundal, E.A. Shaffer, Gallbladder cancer: epidemiology and outcome, Clin. Epidemiol. 6 (2014) 99–109.
[2] N. Razumilava, G.J. Gores, Cholangiocarcinoma. Lancet. 383 (2014) 2168–2179.
[3] B Sr Sahoo, S. Barik, P. Mishra, S.K. Das Majumdar, D.K. Parida, Metastasis to breast from carcinoma gallbladder: a case report and review of literature, Cureus 12 (2020) e11307.
[4] K. Gu, A.M. Wu, B. Yu, T.T. Zhang, X. Lai, J.Z. Chen, H. Yan, P. Zheng, Y.H. Luo, J.Q. Luo, J.N. Pu, Q.Y. Wang, H.F. Wang, D.W. Chen, Iron overload induces colitis by modulating ferroptosis and interfering gut microbiota in mice, Sci. Total Environ. 905 (2023) 167043.
[5] Y.T. Xue, X.J. Jiang, J.R. Wang, Y.X. Zong, Z.N. Yuan, S.S. Miao, X.H. Mao, Effect of regulatory cell death on the occurrence and development of head and neck squamous cell carcinoma, Biomark. Res. 11 (2023) 2.
[6] Y.M. Wang, X.R. Wu, R. Zhao, Y.L. Li, W.L. Zou, J.C. Chen, H.Q. Wang, Overcoming cancer chemotherapy resistance by the induction of ferroptosis, Drug Resist Updat 66 (2023) 100916.
[7] Z.P. Wei, S.H. Hang, D.K. Wiredu Ocansey, Z.Y. Zhang, B. Wang, X. Zhang, F. Mao, Human umbilical cord mesenchymal stem cells derived exosome shuttling mir-129-5p attenuates inflammatory bowel disease by inhibiting ferroptosis, J Nanobiotechnology 21 (2023) 188.
[8] Y. Su, B. Zhao, L. Zhou, Z. Zhang, Y. Shen, H. Lv, L.H.H. AlQudsy, P. Shang, Ferroptosis, a novel pharmacological mechanism of anti-cancer drugs, Cancer Lett. 483 (2020) 127–136.
[9] X. Wu, Y. Li, S. Zhang, X. Zhou, Ferroptosis as a novel therapeutic target for cardiovascular disease, Theranostics 11 (2021) 3052–3059.
[10] D. Tang, X. Chen, R. Kang, G. Kroemer, Ferroptosis: molecular mechanisms and health implications, Cell Res. 31 (2021) 107–125.
[11] H.J. Luo, T. Xiao, X.X. Sun, Y. Song, W.Q. Shi, K.K. Lu, D.Y. Chen, C. Sun, Q. Bian, The regulation of circRNA_kif26b on alveolar epithelial cell senescence via mir-346-3p is involved in microplastics-induced lung injuries, Sci. Total Environ. 882 (2023) 163512.
[12] Y. Zhang, Q.Q. Liu, X.M. Zhang, H.Q. Huang, S.Q. Tang, Y.J. Chai, Z.R. Xu, M.R. Li, X. Chen, J. Liu, C.B. Yang, Recent advances in exosome-mediated nucleic acid delivery for cancer therapy, J Nanobiotechnology 20 (2022) 279.
[13] X. Guo, C. Gao, D.H. Yang, S. Li, Exosomal circular RNAs: a chief culprit in cancer chemotherapy resistance, Drug Resist Updat 67 (2023) 100937.
[14] R.X. Chen, H.L. Liu, L.L. Yang, F.H. Kang, L.P. Xin, L.R. Huang, Q.F. Guo, Y.L. Wang, Circular RNA circRNA_0000285 promotes cervical cancer development by regulating FUS, Eur. Rev. Med. Pharmacol. Sci. 23 (2019) 8771–8778.
[15] Y. Liu, S. Chen, Z.H. Zong, X. Guan, Y. Zhao, CircRNA WHSC1 targets the miR-646/NPM1 pathway to promote the development of endometrial cancer, J. Cell Mol. Med. 24 (2020) 6898–6907.
[16] Z. Liu, Y. Zhou, G. Liang, Y. Ling, W. Tan, L. Tan, R. Andrews, W. Zhong, X. Zhang, E. Song, C. Gong, Circular RNA hsa_circ_001783 regulates breast cancer progression via sponging miR-200c-3p, Cell Death Dis. 10 (2019) 55.
[17] T. Lan, H. Li, D. Zhang, L. Xu, H. Liu, X. Hao, X. Yan, H. Liao, X. Chen, K. Xie, J. Li, M. Liao, J. Huang, K. Yuan, Y. Zeng, H. Wu, KIAA1429 contributes to liver cancer progression through N6-methyladenosine-dependent post-transcriptional modification of GATA3, Mol. Cancer 18 (2019) 186.
[18] J. Lin, X. Peng, K. Dong, J. Long, X. Guo, H. Li, Y. Bai, X. Yang, D. Wang, X. Lu, Y. Mao, X. Sang, X. Ji, H. Zhao, H. Liang, Genomic characterization of co-existing neoplasia and carcinoma lesions reveals distinct evolutionary paths of gallbladder cancer, Nat. Commun. 12 (2021) 4753.

[19] R. Lam, A. Zakko, J.C. Petrov, P. Kumar, A.J. Duffy, T. Muniraj, Gallbladder disorders: a comprehensive review, Dis Mon. 67 (2021) 101130.

[20] G. Lei, L. Zhuang, B. Gan, Targeting ferroptosis as a vulnerability in cancer, Nat. Rev. Cancer 22 (2022) 381–396.

[21] R. Wei, Y. Zhao, J. Wang, X. Yang, S. Li, Y. Wang, X. Yang, J. Fei, X. Hao, Y. Zhao, L. Gui, X. Ding, Tagitinin C induces ferroptosis through PERK-Nrf2-HO-1 signaling pathway in colorectal cancer cells, Int. J. Biol. Sci. 17 (2021) 2703–2717.

[22] D. Wang, G. Wei, J. Ma, S. Cheng, L. Jia, X. Song, M. Zhang, M. Ju, L. Wang, L. Zhao, S. Xin, Identification of the prognostic value of ferroptosis-related gene signature in breast cancer patients, BMC Cancer 21 (2021) 645.

[23] S. Ouyang, H. Li, L. Lou, Q. Huang, Z. Zhang, J. Mo, M. Li, J. Lu, K. Zhu, Y. Chu, W. Ding, J. Zhu, Z. Lin, L. Zhong, J. Wang, P. Yue, J. Turkson, P. Liu, Y. Wang, X. Zhang, Inhibition of STAT3-ferroptosis negative regulatory axis suppresses tumor growth and alleviates chemoresistance in gastric cancer, Redox Biol. 52 (2022) 102317.

[24] G.N. He, N.R. Bao, S. Wang, M. Xi, T.H. Zhang, F.S. Chen, Ketamine induces ferroptosis of liver cancer cells by targeting lncRNA PVT1/miR-214-3p/GPX4, Drug Des Devel Ther 15 (2021) 3965–3978.

[25] S. Wang, Y. Zhang, Q. Cai, M. Ma, L.Y. Jin, M. Weng, D. Zhou, Z. Tang, J.D. Wang, Z. Quan, Circular RNA FOXP1 promotes tumor progression and Warburg effect in gallbladder cancer by regulating PKLR expression, Mol. Cancer 18 (2019) 145.

[26] Y. Qin, Y. Zheng, C. Huang, Y. Li, M. Gu, Q. Wu, Knockdown of circSMAD2 inhibits the tumorigenesis of gallbladder cancer through binding with eIF4A3, BMC Cancer 21 (2021) 1172.